ACS Catalysis

Research Article

pubs.acs.org/acscatalysis

DFT Mechanistic Study of Ru^{II}-Catalyzed Amide Synthesis from Alcohol and Nitrile Unveils a Different Mechanism for Borrowing Hydrogen

Chunyu Song,[†] Shuanglin Qu,[†] Yuan Tao,[†] Yanfeng Dang,[†] and Zhi-Xiang Wang*[,†,‡]

[†]School of Chemistry and Chemical Engineering, University of the Chinese Academy of Sciences, Beijing 100049, China

[‡]Collaborative Innovation Center of Chemical Science and Engineering, Tianjin 300072, China

Supporting Information

ABSTRACT: Using Ru^{II} complex as a mediator, Hong and co-workers recently developed a redox-neutral synthetic strategy to produce amide from primary alcohol and nitrile with complete atom economy. Intrigued by the novel strategy, we performed DFT computations to unravel the catalytic mechanism of the system. The transformation is catalyzed by $Ru^{II}H_2(CO)(PPh_3)(I^iPr)$ (I^iPr = 1,2-diisopropylimidazol-2-ylidene) via four stages including nitrile reduction, alcohol dehydrogenation, C−N coupling, and amide production. Generally, alcohol dehydrogenation in dehydrogenative coupling (DHC) or borrowing hydrogen methodology (BHM) takes place separately, transferring the H^{α} and hydroxyl H^{OH} atoms of alcohol to the catalyst to form the catalyst-H_2 hydride. Differently, the alcohol dehydrogenation in the present system couples with nitrile hydrogenation; alcohol plays a reductant role to aid nitrile reduction by transferring its H^{OH} to nitrile N atom directly and H^{α} to the catalyst and meanwhile becomes partially oxidized. In our proposed preferred mechanism-B, the Ru^{II} state of the catalyst is retained in the whole catalytic cycle. Mechanism-A, postulated by experimentalists, involves $Ru^{II} \rightarrow Ru^{0} \rightarrow Ru^{II}$ oxidation state alternation, and the Ru^{0} intermediate is used to dehydrogenate alcohol separately via oxidative addition, followed by β-hydride elimination. As a result, mechanism-B is energetically more favorable than mechanism-A. In mechanism-B, the (N-)H atom of the amide bond exclusively originates from the hydroxyl H^{OH} of alcohol. In comparison, the (N-)H atom in mechanism-A stems from either H^{OH} or H^{α} of alcohol. The way of borrowing hydrogen that is used by nitrile is via participating in alcohol dehydrogenation, which is different from that in the conventional DHC/BHM reactions and may help expand the strategy and develop new routes for utilizing DHC and BHM strategies.

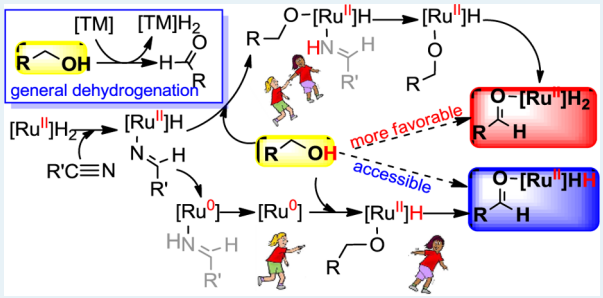

KEYWORDS: *DFT computations, dehydrogenative coupling, borrowing hydrogen methodology, acceptorless dehydrogenation, amide synthesis, alcohol dehydrogenation*

1. INTRODUCTION

Development of green and atom-economic molecular transformations[1] is a focal point of contemporary chemical research, due to the depletion of the reserve of fossil-based feedstock and environmental concerns. Among others, dehydrogenative coupling (DHC)[2] through acceptorless dehydrogenation (AD),[3] also known as borrowing hydrogen methodology (BHM)[4] is an active area of study. This methodology has been applied to synthesize chemicals such as amides,[5] imines,[6] esters,[2c,7] and pyrroles[8] and to carry out alkane metathesis reactions.[3e,9]

The amide bond is a ubiquitous linkage in biological molecules and natural products[10,11] and is often used to construct pharmaceutical molecules.[12] There has been a great demand to develop novel methodology to synthesize amides, but the conventional synthetic routes[13−15] do not meet the standards of green chemistry, because these often require harsh conditions and produce chemical wastes. In 2007, Milstein and co-workers made a breakthrough, discovering that the PNN-Ru pincer complex (**1**) could mediate amide synthesis from amines and primary alcohols (eq 1) under mild conditions with only

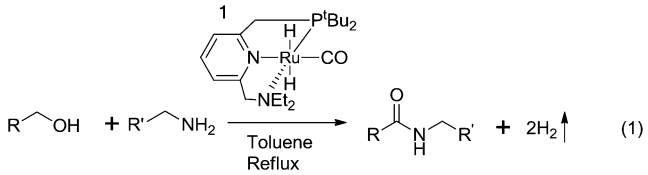

(1)

H_2 released as a byproduct, without using a stoichiometric activating agent.[5a] Subsequent to this seminal work, there have been several reports of similar amide-forming reactions catalyzed by different transition metal complexes,[8a,16−20] among which Zeng and Guan have reported the synthesis of

Received: June 12, 2014
Revised: July 18, 2014
Published: July 21, 2014

   dx.doi.org/10.1021/cs5008156 | ACS Catal. 2014, 4, 2854−2865

polyamides from diols and diamines, using the same catalyst (**1**).[21]

The novelties of AD reactions and AD-based couplings have triggered many computational studies to gain insight into the detailed mechanisms.[22,23] Relevant to the present work are our previous work wherein we investigated the catalytic mechanisms of amide[23a] and imine[23e] synthesis from primary alcohol and amine, catalyzed by **1**[5a,21] and PNP-Ru pincer complex,[6,24] respectively, and pyrrole from secondary alcohol and β-amino alcohol,[23g] catalyzed by PNP-Ir[25] and PNN-Ru (an analogue of **1**) pincer complexes, respectively. In this context, we were attracted by a novel amide synthesis from primary alcohol and nitrile (eq 2), recently reported by Hong and co-workers.[26]

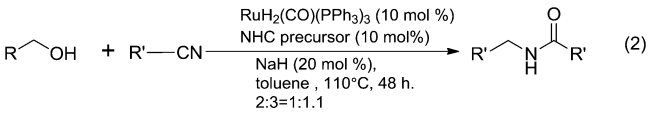

(2)

Different from eq 1, the hydrogen from alcohol dehydrogenation in eq 2 is not released but is used to reduce nitrile. Thus, eq 2 is redox-neutral with complete atom economy.

Exemplified by Scheme 1(A), a DHC/BHM reaction includes two key steps: AD to activate the alcohol to more reactive ketone or aldehyde and coupling of ketone or aldehyde with its partner to finally form a more stable product. Hong et al. postulated a mechanism (namely, mechanism-A) to rationalize their transformations (Scheme 1B).[26] In their mechanism, the alcohol dehydrogenation (stage II) takes place separately, mediated by a Ru^0 intermediate, which is similar to the dehydrogenation in DHC/BHM reactions, as compared by the blue segments in Scheme 1A and B. However, as will be discussed, mechanism-A is not consistent with the deuterium-labeling experiment (Scheme 3 in ref 26). We envisaged that their reactions may furnish a different mechanism, which encouraged us to perform a deep mechanistic study to unveil the mechanism hidden from the experimental discovery.

2. COMPUTATIONAL DETAILS

For a catalytic system, both geometric and electronic structures of the catalyst and substrates have profound influences on both catalytic mechanism and efficiency. Thus, we used actual catalyst and substrates rather than truncated models in mechanistic computations. All reported structures were optimized and then characterized to be minima without imaginary frequency or transition states (TSs) having a unique imaginary frequency at B3LYP[27]/BSI level in the gas phase, BSI designating a basis set combining SDD[28] for Ru and 6-31G(d,p)[29] for nonmetal atoms. The energies were further improved by single-point calculations at the M06[30]/BSII//B3LYP/BSI level with solvation effects accounted for by the SMD[31] model, using experimental solvent (toluene). BSII denotes a basis set combining SDD for Ru and 6-31++G(d,p)[32] for nonmetal atoms. The M06//B3LYP combination has been applied in many computational studies of various catalytic systems by others and us.[33] The gas phase B3LYP/BSI harmonic frequencies were employed for thermal and entropic corrections to the enthalpies and free energies at 298.15 K and 1 atm. It should be emphasized that such corrections based on the ideal gas phase model inevitably overestimate entropy contributions to free energies for reactions in solvent, in particular for reactions involving multicomponent changes, because of ignoring the suppressing effect of solvent on the rotational and transitional freedoms of substrates. The entropy overestimation by the ideal gas phase model was also demonstrated by experimental studies.[34] Since no standard quantum mechanics-based approach is available to accurately calculate entropy in solution, we adopted the approximate approach proposed by Martin et al.[35] According to their approach, a correction of 4.3 kcal/mol applies for a component change for a reaction at 298.15 K and 1 atm (i.e., a reaction from m- to n-components has an additional correction of $(n - m) \times 4.3$ kcal/mol). Previously, we applied the correction protocol for mechanistic studies of various catalytic reactions and found that such corrected free energies were more reasonable than enthalpies and uncorrected free energies, although the protocol is by no means accurate.[23c,d,36] In the following, we discuss the mechanism in terms of the corrected free energies and give the enthalpies for reference in the brackets in the relevant schemes. All standard calculations were carried out using the Gaussian 09 program.[37] Total energies and Cartesian coordinates of all optimized structures are given in Supporting Information (SI).

3. RESULTS AND DISCUSSION

Hong et al.[26] have applied their strategy to synthesize amides from various primary alcohols and nitriles. Using eq 3 as a standard reaction, they optimized a catalytic condition (see eq

Scheme 1. (A) Examples of General Catalytic Mechanisms for DHC (blue and black)/BHM (blue and pink) Reactions; (B) Experimentally Postulated Mechanism for Amide Synthesis from Alcohol and Nitrile

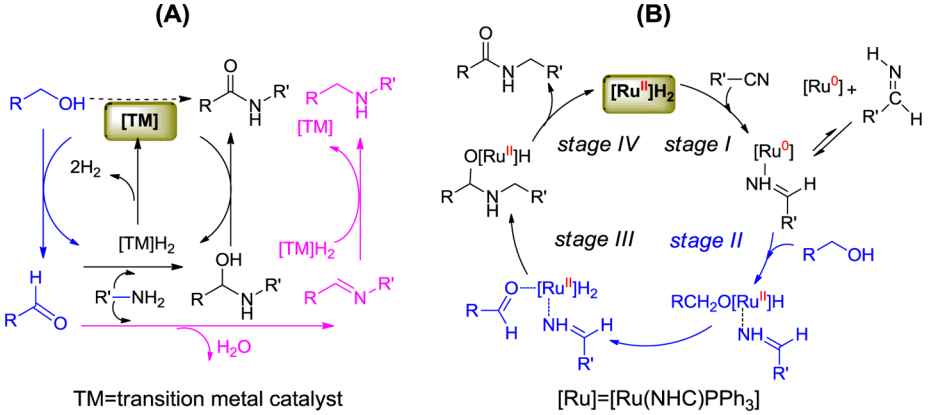

dx.doi.org/10.1021/cs5008156 | ACS Catal. 2014, 4, 2854−2865

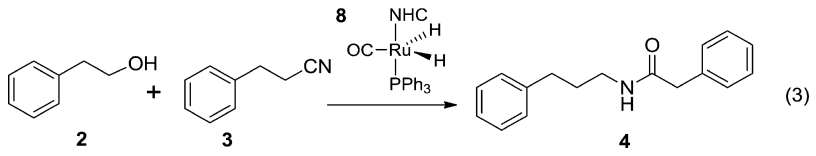

Scheme 2. Free Energy Profiles for Nitrile Reduction (stage I), along with Enthalpies (in brackets); Optimized Geometries of Key Stationary Points Are Displayed in Figure 1

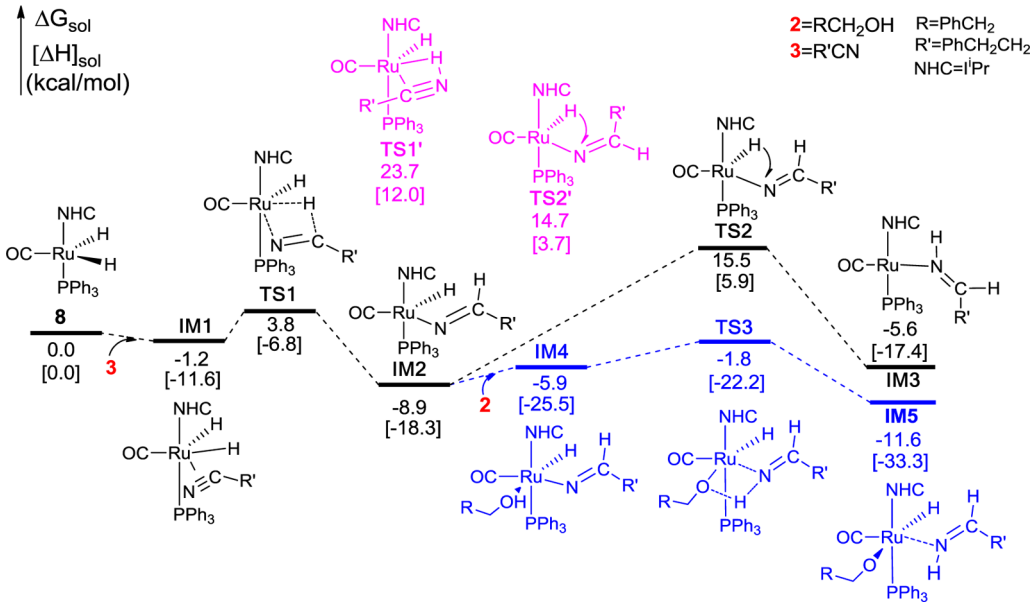

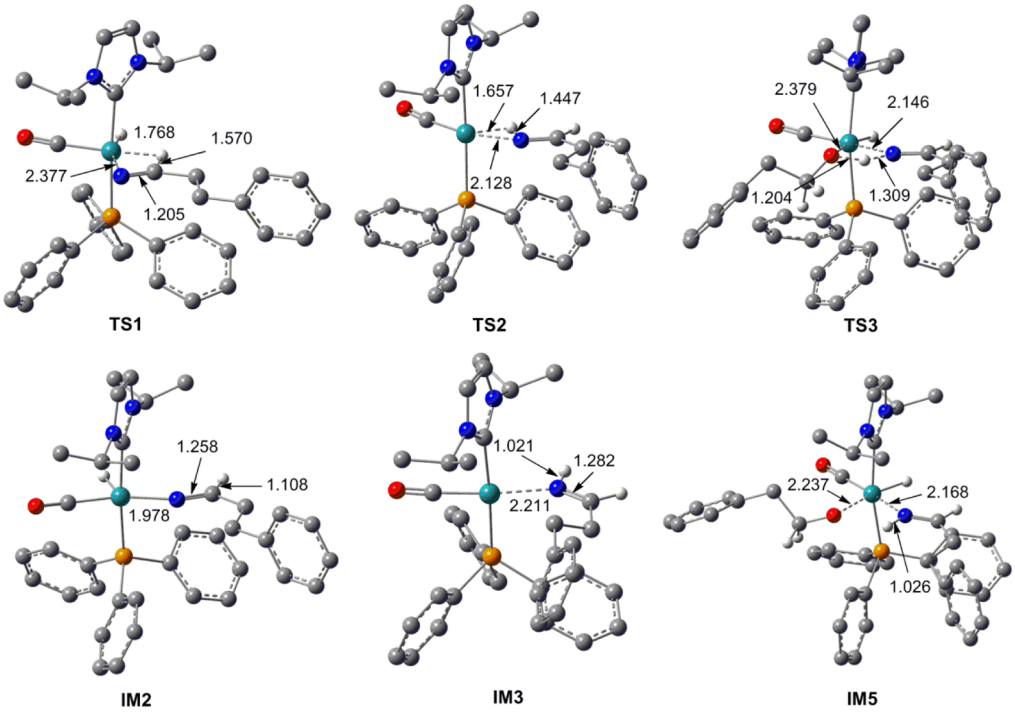

Figure 1. Optimized structures of the key stationary points labeled in Scheme 1. Key bond lengths are given in Å, and trivial H atoms are omitted for clarity.

2) and investigated the catalytic mechanism. The NMR experiment showed that the catalytic system involved two new Ru hydrides in addition to the $Ru^{II}H_2(CO)(PPh_3)_3$ precursor (**5**). The two new hydrides were assigned to $Ru^{II}H_2(CO)(PPh_3)_2(I^iPr)$ (I^iPr = 1,2-diisopropylimidazol-2-ylidene) **6** and $Ru^{II}H_2(CO)(PPh_3)(I^iPr)_2$ **7**, respectively. Furthermore, they demonstrated that the $Ru^{II}H_2(CO)(PPh_3)_2(I^iPr)$ complex (**6**) prepared separately was also equally effective to promote the eq 3 reaction. Because **6** is an 18*e* octahedral complex saturated electronically and coordinatively,

dx.doi.org/10.1021/cs5008156 | ACS Catal. 2014, 4, 2854−2865

Scheme 3. Free Energy Profiles for Alcohol Dehydrogenation (stage II), along with Enthalpies (in brackets); Optimized Geometries of Key Stationary Points Are Displayed in Figure 2

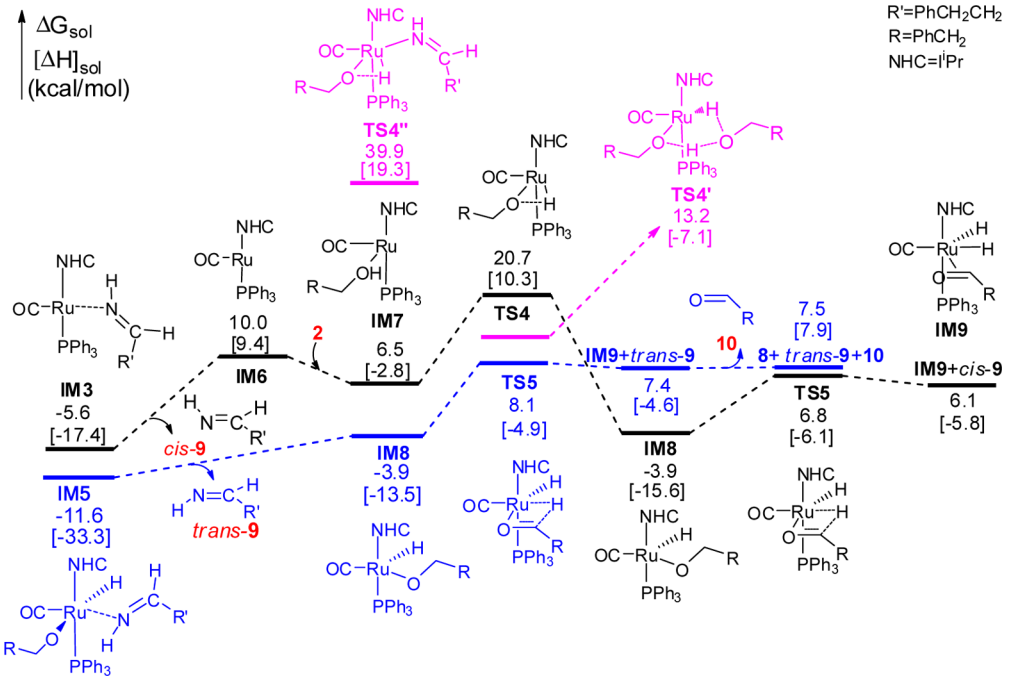

a PPh_3 ligand should dissociate from **6** to generate an active catalyst (i.e., ($Ru^{II}H_2(CO)(PPh_3)(I^iPr)$ **8**) which is a 16*e* Ru^{II} complex with a vacant coordination site. The moderate dissociation energy (15.3 kcal/mol) indicates that **8** could exist via equilibrium under the catalytic conditions (T = 110.0 °C). Thus, we used **8** as the real catalyst to compute the mechanism for the eq 3 transformation. The optimized structures of complexes **5**, **6**, 7, and **8** are given in Figure S1 in the SI.

The mechanism-A (Scheme 1B) can be characterized by four stages, including nitrile hydrogenation to imine (stage I), alcohol dehydrogenation to aldehyde (stage II), C−N coupling (stage III), and amide production and catalyst regeneration (stage IV). Our computed mechanism (namely, mechanism-B) is different from mechanism-A, but schematically similar. In the following we detail the catalytic pathway for mechanism-A in terms of the four stages, and meanwhile disclose our proposed mechanism-B.

Nitrile Reduction to Imine (Stage I). Scheme 2 illustrates the pathways for nitrile reduction to imine, together with the energetic results. Figure 1 displays the optimized structures of the key stationary points labeled in Scheme 2. The reduction begins by inserting the C≡N bond of nitrile (**3**) to one of the Ru−H bonds of the dihydride catalyst (**8**). After forming a weak complex **IM1** (ΔG = −1.2 kcal/mol) with **8**, the insertion of **3** takes place by spanning **TS1** and leads to **IM2**. The relative energies of **TS1** (3.8 kcal/mol) and **IM2** (−8.9 kcal/mol) indicate the easiness of the process. **TS1**′ (see Figure S2 in the SI for its optimized structure) for inverse C≡N insertion is 19.9 kcal/mol higher than **TS1**. Subsequent to the insertion, two possible pathways were examined to complete the reduction. According to mechanism-A (Scheme 1A), the black pathway continues to transfer the remaining (Ru-)H atom to the N atom through **TS2**, leading to the Ru-bound imine complex (**IM3**). Relative to **IM2**, the H-transfer crosses a barrier of 24.4 kcal/mol (**TS2**) and is endergonic by 3.3 kcal/mol. The imine part in **IM3** is in *cis* conformation, but Hong et al. observed the NMR signal of *trans*-imine.[26] We located **TS2**′ (see Figure S2 in the SI for its optimized structure) to give *trans*-imine, and it is energetically comparable with **TS2**.

As the energetic results indicate that the above nitrile hydrogenation step in mechanism-A is feasible, we were able to locate a more favorable pathway (the blue one) for nitrile hydrogenation. Because **IM2** is a 16*e* Ru^{II} complex with a vacant coordination site, the alcohol substrate **2** can coordinate to its Ru^{II} center, forming a complex **IM4**. The coordination is downhill by 7.2 kcal/mol in enthalpy but uphill by 3.0 kcal/mol in free energy due to the entropy penalty. Nevertheless, the hydroxyl H^{OH} of **2** in **IM4** can readily transfer to the N atom via a four-membered TS (**TS3**), resulting in a more stable complex, **IM5**. In **TS3**, the distances of the breaking O−H bond (1.204 Å) and forming N−H bond (1.309 Å) confirm the H-transfer process geometrically. Relative to **IM2** + **2**, the process crosses a barrier of 7.1 kcal/mol and is exergonic by 2.7 kcal/mol. The blue pathway is more favorable than the black one in terms of both kinetics and thermodynamics; **TS3** and **IM5** in the former are 17.3 and 6.0 kcal/mol lower than their counterparts (**TS2** and **IM3**) in the latter, respectively. The preference of the blue pathway over the black one is understandable, because the nitrile reduction along the blue pathway does not change the oxidation state of Ru^{II}, whereas that along the black pathway involves a $Ru^{II} \rightarrow Ru^0$ alteration. In addition, the N center serves as a Lewis base to help alcohol deprotonation in **TS3**, which is in contrast to a hydridic (Ru-)H transfer to the N center in **TS2**. Thus, alcohol **2** in the blue pathway plays a reductant role to aid the nitrile reduction. The differences between **IM3** and **IM5** resulting from the two mechanisms, respectively, include the following: (i) **IM3** and **IM5** are Ru^0 and Ru^{II} complexes, respectively, (ii) the imine parts in **IM3** and **IM5** have *cis* and *trans* conformations, respectively, and (iii) alcohol **2** in **IM5** is partially oxidized.

dx.doi.org/10.1021/cs5008156 | ACS Catal. 2014, 4, 2854−2865

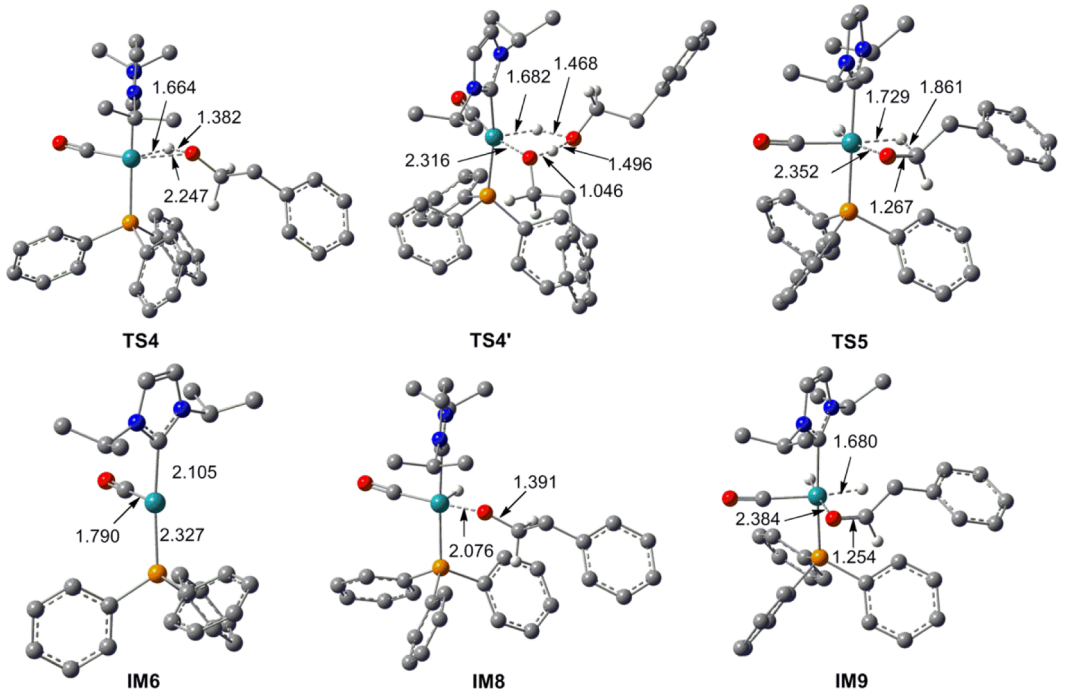

Figure 2. Optimized structures of the key stationary points labeled in Scheme 2. Key bond lengths are given in Å, and trivial H atoms are omitted for clarity.

Scheme 4. Free Energy Profiles for C−N Coupling (stage III), along with Enthalpies (in brackets); Optimized Geometries of Key Stationary Points Are Displayed in Figure 3

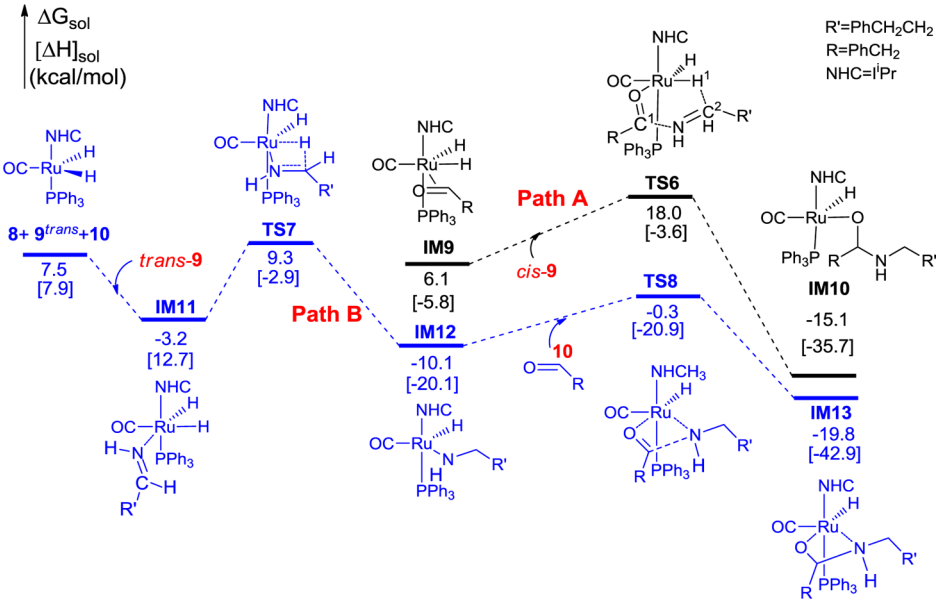

Alcohol Oxidation to Aldehyde *(Stage II)*. Alcohol dehydrogenation activates alcohol to more reactive ketone/aldehyde, which is a crucial step in DHC/BHM reactions using alcohol as a coupling partner. In general, alcohol dehydrogenation occurs separately (Scheme 1A), e.g. those in amide,[5,23a] imine,[6,23e] and pyrrole[8,38b] synthesis. Beginning with **IM3** and **IM5** resulting from the black and blue pathways in Scheme 2, respectively, Scheme 3 depicts the pathways for alcohol oxidation, together with the energetic results. Figure 2 displays the optimized structures of key stationary points labeled in Scheme 3.

The black pathway follows mechanism-A. **IM3** first transforms to a 14*e* three-coordination Ru^0 complex (**IM6**) by releasing imine (*cis*-**9**). Subsequently, **IM6** serves as a reductant to dehydrogenate alcohol **2**, which proceeds through oxidative addition (**IM6** + **2** → **IM7** → **TS4** → **IM8**), followed by *β*-H elimination (**IM8**→ **TS5** → **IM9**). Similar to previous findings,[23d,38] a proton shuttle (e.g., alcohol **2**) facilitates the oxidative addition greatly; **TS4′** is 7.5 kcal/mol lower than **TS4**. The process activates alcohol to a Ru-bound aldehyde complex (**IM9**). Measured from **IM3** + **2**, the effective barrier for the alcohol oxidation step is 18.8 kcal/mol (**TS4′**), and the process is endergonic by 11.7 kcal/mol.

dx.doi.org/10.1021/cs5008156 | ACS Catal. 2014, 4, 2854−2865

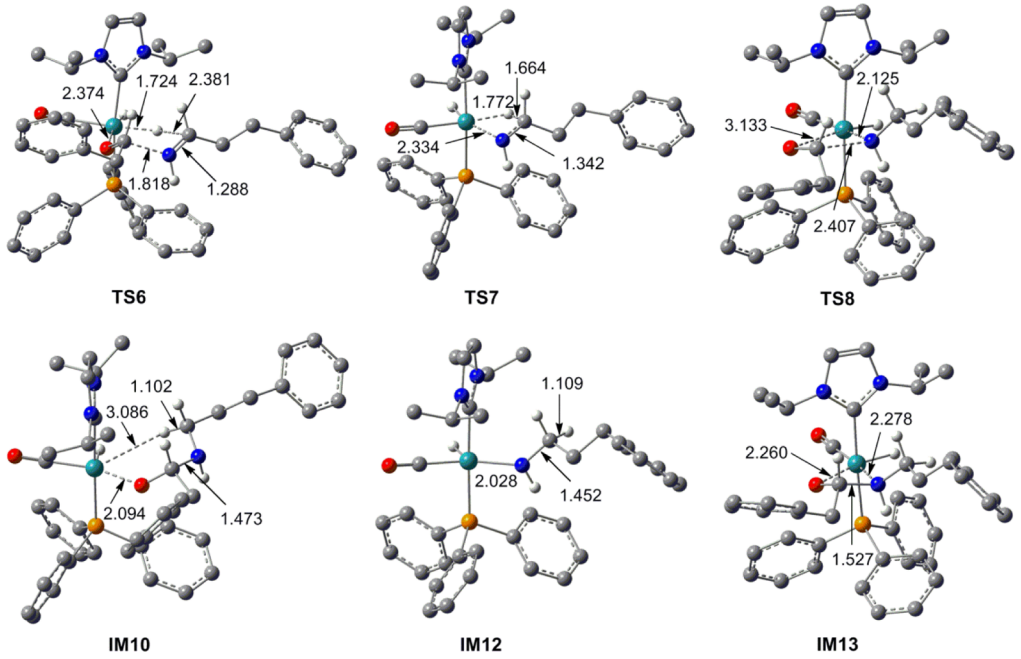

Figure 3. Optimized structures of the key stationary points labeled in Scheme 4. Key bond lengths are given in Å, and trivial H atoms are omitted for clarity.

Scheme 5. Free Energy Profiles for C−N Coupling (Path C for stage III), along with Enthalpies (in brackets); Optimized Geometries of Key Stationary Points Are Displayed in Figure 4

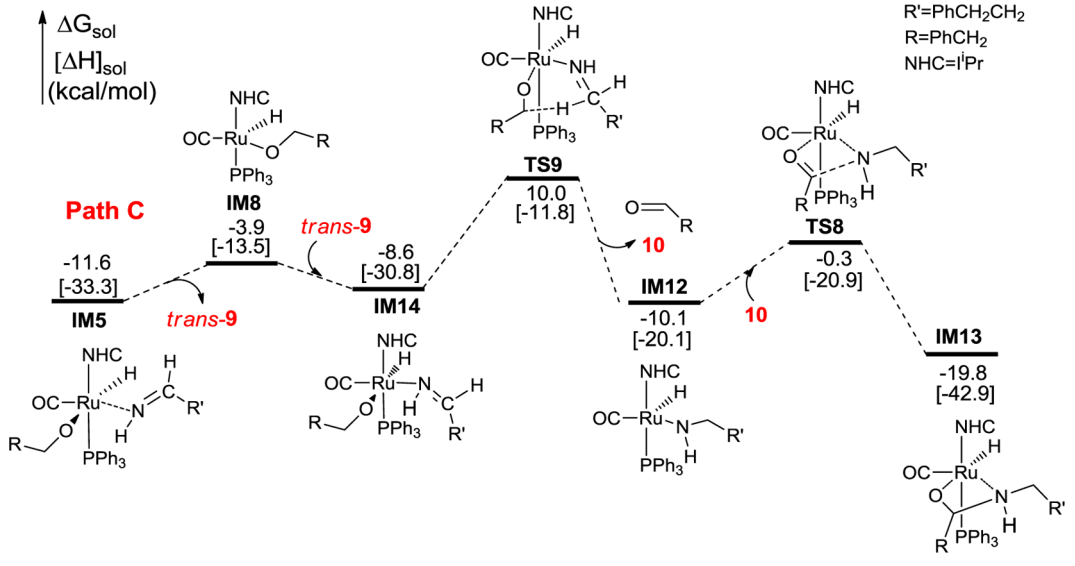

The alcohol dehydrogenation is mediated by **IM6**. Because the formation of **IM6** from **IM3** costs 15.6 kcal/mol, we thus further examined if **IM3** can mediate the process directly. The barrier (**TS4′′**) for alcohol **2** oxidative addition to **IM3** is 39.9 kcal/mol, which is much higher than **TS4** and **TS4′**, excluding the possibility.

Starting from **IM5** is led by the blue pathway in Scheme 2, and because alcohol **2** is already involved in the nitrile reduction (stage I) and becomes partially oxidized in **IM5**, this stage in mechanism-B is only to complete alcohol oxidation. Release of *trans*-imine (*trans*-**9**) from **IM5** results in **IM8**. Then the vacant active site in **IM8** promotes *β*-H elimination through **TS5**, giving the same Ru-bound aldehyde (**IM9**) as that in the black pathway. Note that, because the different imine conformations (*cis*-**9** vs *trans*-**9**) are involved in the two pathways, there is a slight energetic difference between *cis*-**9** + **IM9** and *trans*-**9** + **IM9**. Relative to **IM5**, the effective barrier for this process is 19.7 kcal/mol and the process is endergonic by 19.1 kcal/mol.

C−N Coupling (Stage III). On the basis of the species generated from stages I and II, we examined four pathways for C−N coupling below, namely Paths A−D, respectively.

On the basis of mechanism-A, the black pathway (Path A) in Scheme 4 describes the C−N bond formation process, starting from **IM9** and *cis*-**9** resulting from the black pathway in Scheme 3. **TS6** illustrates the C−N bond formation via the attack of the nucleophilic N center of *cis*-**9** to the carbonyl carbon (C^1) of aldehyde part in **IM9**. In **TS6**, the C^1−N bond length is 1.818

dx.doi.org/10.1021/cs5008156 | ACS Catal. 2014, 4, 2854−2865

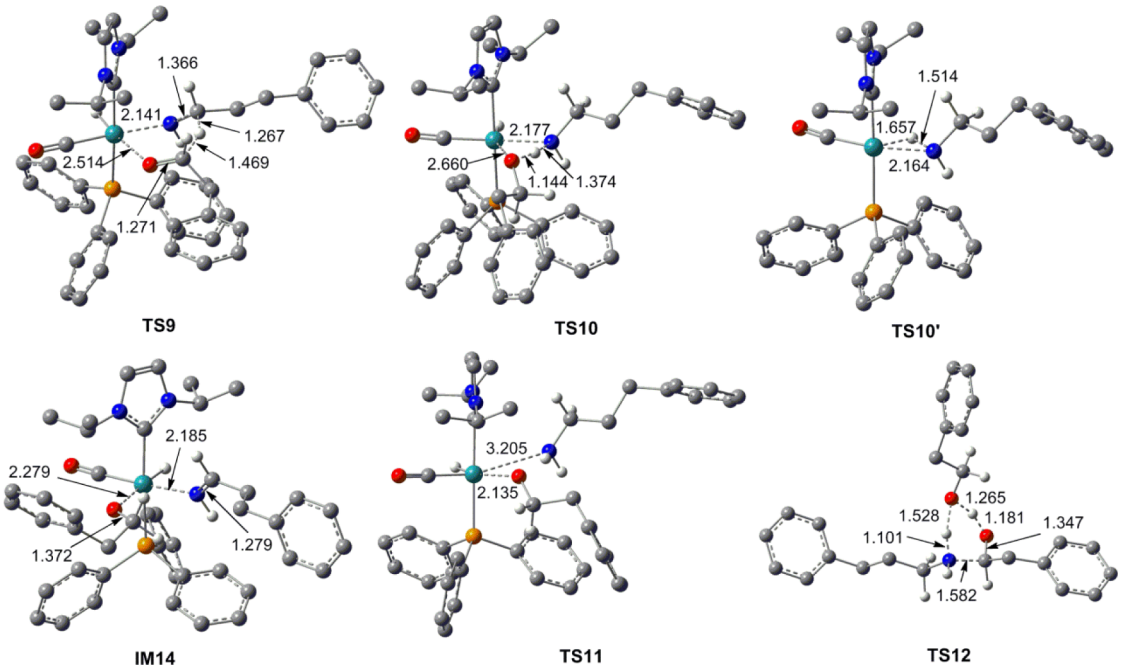

Figure 4. Optimized structures of the key stationary points labeled in Scheme 5 and Scheme6. Key bond lengths are given in Å and trivial H atoms are omitted for clarity.

Scheme 6. Free Energy Profile for C−N Coupling (Path D for stage III), along with Enthalpies (in brackets); Optimized Geometries of Key Stationary Points Are Displayed in Figure 4

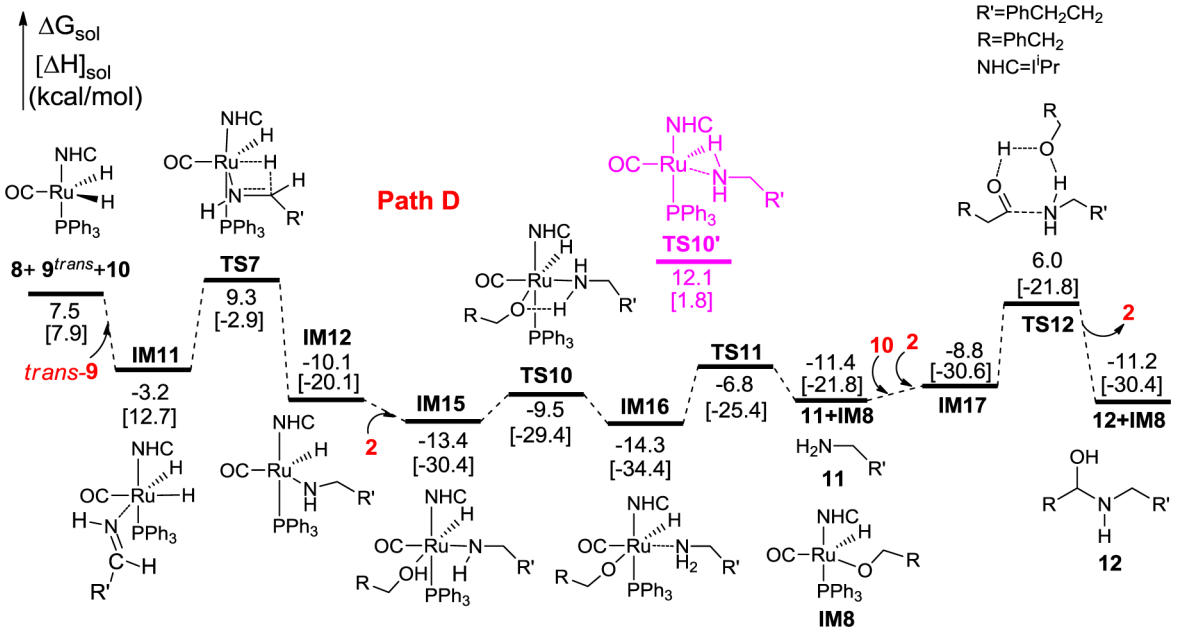

Å and the distances of Ru−H^1 and H^1···C^2 in Ru−H^1···C^2 are 1.724 and 2.381 Å, respectively, indicating that C^1−N bond is forming but the C^2−H^1 bond formation is elongated. However, because the attack results in a carbocation center (C^2) on the *cis*-**9** part, the hydridic H^1 on Ru can migrate to C^2 easily forming the C^2−H^1 bond, leading **TS6** to **IM10** directly. Because no TS and intermediate for the H^1 migration could be located, we speculate that the formations of C^1−N and C^2−H^1 and the breaking of Ru−H^1 is actually a concerted process, although **TS6** does not look like a concerted TS geometrically. Relative to **IM9** + *cis*-**9**, the C−N coupling crosses a barrier of 11.9 kcal/mol and is exergonic by 21.2 kcal/mol.

The blue pathway (Path B) in Scheme 4 illustrates how the C−N coupling proceeds, starting from liberated *trans*-**9** and aldehyde (**10**), mediated by the active catalyst **8**. First *trans*-**9** coordinates to **8** to form **IM11**, followed by the insertion of *trans*-**9** to Ru−H bond via **TS7**, resulting in **IM12**. Then the aldehyde (**10**) attacks **IM12** via **TS8**, leading to **IM13** with the C−N bond formed. In addition to forming the C−N bond, the process forms the Ru−O covalent bond and turns the Ru−N covalent bond to a coordination Ru ← N bond. Consistently, as shown in Figure 3, from **TS8** to **IM13**, the forming C−N and Ru−O bonds are shortened from 2.407 to 1.527 Å and 3.133 to 2.260 Å, respectively, while the Ru−N bond is slightly

dx.doi.org/10.1021/cs5008156 | ACS Catal. 2014, 4, 2854−2865

elongated from 2.125 to 2.278 Å. Relative to **8** + *trans*-**9** + **10**, the C−N coupling is exergonic by 27.3 kcal/mol.

The third pathway (Path C), starting from **IM5** in Scheme 2, is described in Scheme 5. First, *trans*-**9** liberates from **IM5**, leading to **IM8**, then free *trans*-**9** imine coordinates to **IM8** in another mode, giving **IM14**. Although **IM14** is 3.0 kcal/mol less stable than **IM5**, it allows an intramolecular H-transfer, as described by **TS9**, transferring the H^{β} atom of $[Ru^{II}]-OC^{\beta}H_2R$ to the C^{β} of $[Ru^{II}] \leftarrow NHC^{\beta}HR'$. In **TS9** (Figure 4), the breaking and forming C−H bond lengths are 1.469 and 1.267 Å, respectively. Geometric optimization with an initial structure displaced from **TS9** along the forward direction shows that the aldehyde part can dissociate easily to give **IM12** + **10**. Subsequently, the liberated aldehyde (**10**) attacks the Ru−N bond of **IM12** via **TS8**, resulting in the same complex (i.e., **IM13**) as that in Scheme 4.

Previously, we have computationally found that the C−N bond formation in eq 1 takes place by coupling aldehyde and amine.[23a] Applying the mechanism to the present reaction, the imine requires further reduction to the amine. Scheme 6 details the pathway (Path D) on the basis of the mechanism, starting from **8** + *trans*-**9** + **10**. Compared to the nitrile reduction (Scheme 2), it can be observed that the imine (*trans*-**9**) reduction prefers the mechanism similar to that of nitrile (**3**) reduction. Without repeating the details, we call attention to the fact that the pathway (from **IM12** to **11** + **IM8**) involving alcohol as a reductant is also significantly more favorable than that via sequentially transferring two (Ru-)H atoms of **8** to *trans*-**9** via **TS10** and **TS11**, respectively; **TS10′** is 21.6 and 18.9 kcal/mol higher than **TS10** and **TS11**, respectively. After amine (**11**) is formed, aldehye (**10**) couples with amine (**11**) to form a C−N bond. Either water or alcohol can accelerate the C−N coupling. According to our previous finding[23g] that alcohol is more effective to facilitate the C−N coupling, we used alcohol as a mediator to estimate the coupling barrier as shown by **TS12**. The coupling results in hemiaminal **12** which can further be transformed to amide product **4** (see Scheme S1 in SI).

The relative energies of the highest TSs in Paths A−D are 18.0 (**TS6**), 9.3 (**TS7**), 10.0 (**TS9**), and 9.3 kcal/mol (**TS7**). The relative energies of formed complexes from the four pathways are −15.1 (**IM10**), −19.8 (**IM13**), −19.8 (**IM13**), −11.2 kcal/mol (**IM8** + **12**). The energetic results indicate the blue Path B in Scheme 4 is most favorable for the C−N bond formation. However, because **TS9** is only 0.7 kcal/mol higher than **TS7**, considering the small energy difference and the inaccuracy of the computational method, Path C should be considered as a possible alternative. Path B and Path D share the highest **TS7**, but because **TS8** in path B is 6.3 kcal/mol lower than **TS12** in Path D, Path D is unlikely, in agreement with the experimental fact that no amine was observed.

Amide Release and Catalyst Regeneration *(Stage IV)*. Subsequent to stage III, stage IV delivers the finial amide product (**4**) and in the meantime recovers the catalyst (**8**). Starting from **IM10** and **IM13** obtained according to mechanisms-A and -B, respectively, Scheme 7 illustrates the pathways for this stage. **IM10** has a vacant site, meeting the requirement for β-H elimination. However, the C−H^{β} bond in **IM10** is not in the proper position for β-H elimination. Attempts to locate a continuous pathway for the β-H elimination (which may involve stepwise or concerted rotations around multibonds because of the long chain of substrates) were not successful. However, with properly preset initial structures, we were able to obtain β-H elimination TSs to

Scheme 7. Free Energy Profile for C−N Coupling (Path C for stage III), along with Relative Free Energies and Enthalpies (in brackets) in kcal/mol; Optimized Geometries of Key Stationary Points Are Displayed in Figure 5

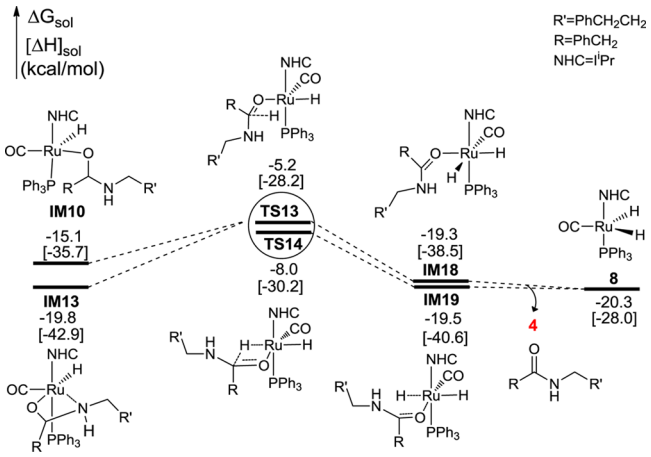

produce amide, exemplified by **TS13** and **TS14**. Measured from **IM10**, the barriers from **IM12** to either **TS13** or **TS14** are not high (<15.0 kcal/mol). **TS13** and **TS14** lead to **IM18** and **IM19**, respectively, from which amide **4** can be liberated and **8** can be regenerated, closing the catalytic cycle. In **IM13**, the Ru−O is a covalent bond and Ru ← N bond is a coordination bond. Thus, **IM13** can undergoes N-dissociation to generate a vacant site for β-H elimination. Similar to the case of **IM10**, we were not able to locate a continuous pathway to reach **TS13** and **TS14** from **IM13**.

Putting the four stages together, we estimate the rate-determining barriers for the entire transformation. Along the blue pathway (Schemes 2−4) for mechanism-B, **IM5** is the lowest intermediate (prior to **IM13**) and **TS7** is the highest TS; thus, the rate-determining barrier is 20.9 kcal/mol. Note that **TS5** is only 1.2 kcal/mol lower than **TS7**. Along the black pathway for mechanism-A, **IM2** is lowest and **TS6** is highest (note that **TS2** is only 2.5 kcal/mol lower than **TS6**); thus, the rate-determining barrier appears to be 26.9 kcal/mol. However, because the formation of **IM5** in stage I is much more favorable than the formation of **IM3**, the actual rate-determining barrier for mechanism-A should be measured from **IM5**, being 29.6 kcal/mol (the energy difference between **IM5** and **TS6**). The comparison indicates mechanism-B is overall more favorable than mechanism-A. Seemingly, our computed rate-determining barrier (20.9 kcal/mol, which is not high) for mechanism-B is not consistent with the temperature (110.0 °C) applied for these transformations. However, it should be noted that the active catalyst **8** is 15.3 kcal/mol less stable than **6** and **8** can only be obtained via equilibrium of **6** ⇌ **8** + PPh_3. Applying a relatively high temperature would help increase the concentration of active catalyst (**8**), thus improving catalysis of the system. In other words, the relatively high reaction temperature is not necessary for the **8**-catalyzed reaction but for producing a substantial amount of **8**. The whole transformation from **2** (alcohol) and **3** (nitrile) to amide (**4**) is exergonic by 20.3 kcal/mol, which is the thermodynamic driving force of the catalytic transformation.

Scheme 8 schematically compares the Hong et al. proposed mechanism-A and our computed mechanism-B, with major intermediates and TSs included. The differences between the two mechanisms include: (I) In mechanism-A, the nitrile

dx.doi.org/10.1021/cs5008156 | ACS Catal. 2014, 4, 2854−2865

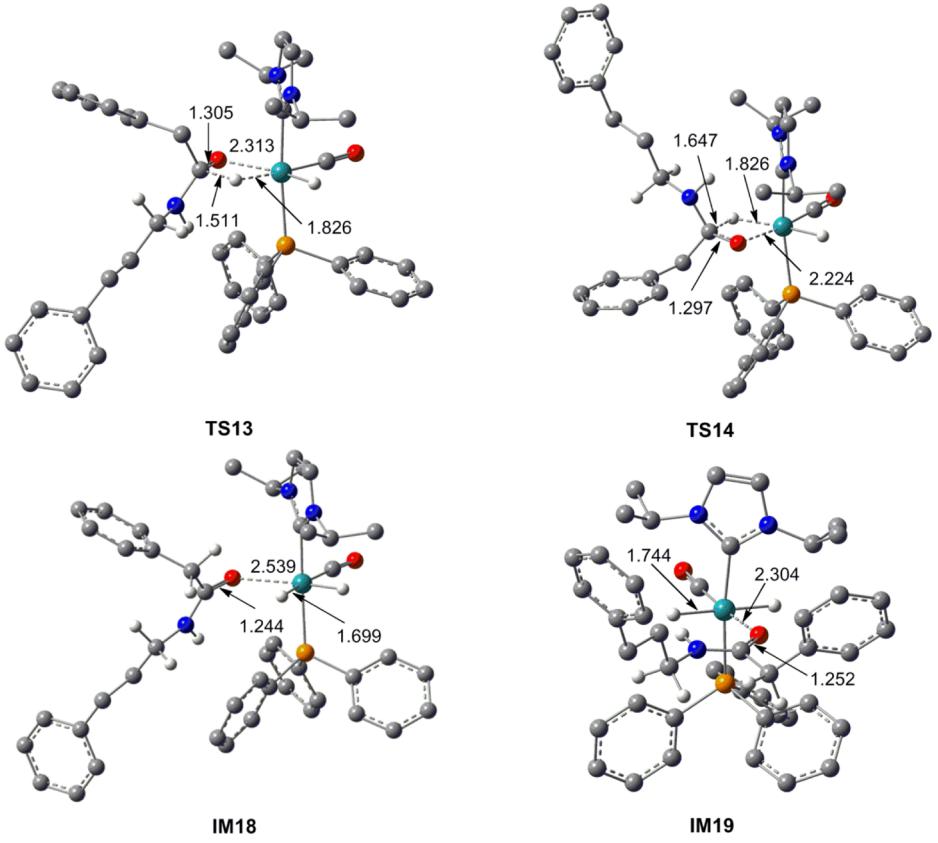

Figure 5. Optimized structures of the key stationary points labeled in Scheme 7 Key bond lengths are given in Å and trivial H atoms are omitted for clarity.

Scheme 8. Comparing the Mechanism-A Postulated by Hong et al. (A) and our Computed Mechanism-B (B)

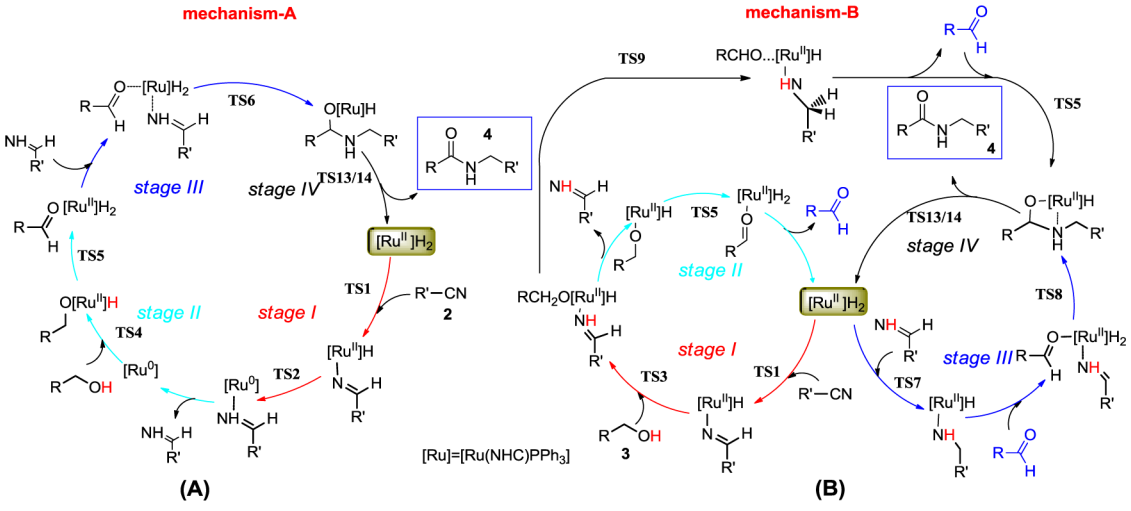

reduction (stage I) and alcohol dehydrogenation (stage II) take place separately, and the reduced Ru^0 complex (**IM6**) from stage I oxidizes alcohol to aldehyde. In contrast, the nitrile reduction and alcohol oxidation in mechanism-B couple together; alcohol **2** plays a reductant role to facilitate the reduction of nitrile, and in the meantime nitrile serves as an oxidant to oxidize alcohol in stage I, and stage II completes the oxidation of partially oxidized alcohol. (II) Mechanism-A involves oxidation state alternation ($Ru^{II} \rightarrow Ru^0 \rightarrow Ru^{II}$), whereas the Ru^{II} oxidation state in mechanism-B is maintained in the whole catalytic cycle. (III) Mechanism-A involves an intermediate of *cis*-imine (*cis*-**9**). Hong et al. proposed that the selectivity of *trans*-imine could be due to the induction of steric hindrance. In comparison, mechanism-B gives *trans*-imine (*trans*-**9**) directly without invoking the induction effect of steric hindrance. Because *trans*-**9** is 1.3 kcal/mol less stable than *cis*-**9**, the observation of *trans*-**9** with higher energy is an evidence for mechanism-B. (IV) The (N-)H atom of the amide bond in mechanism-B exclusively originates from the hydroxyl H^{OH} of alcohol via **TS3** in stage I (Scheme 2) and the H^{α} atom of alcohol **2a** does not transfer to the N atom. In mechanism-A, both the hydroxyl H^{OH} and H^{α} atoms of **2a** transfer to the Ru

dx.doi.org/10.1021/cs5008156 | ACS Catal. 2014, 4, 2854−2865

center via **TS4** and **TS13**/**TS14**, respectively. Therefore, as the transformation goes on, the active catalyst **8** becomes a Ru dihydride with H atoms coming from hydroxyl H^{OH} and H^{α} of alcohol. The H-transfer in mechanism-B is consistent with the NMR results (eq 4) reported in ref 26, which shows no

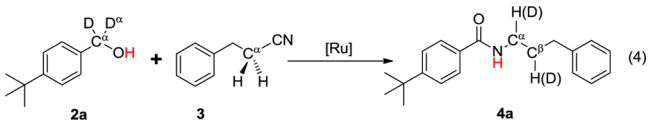

(4)

deuteration on the NH of amide bond. A reviewer kindly reminded us that NaH may also mediate deuteration on the NH of amide bond, which was not analyzed by experimentalists. However, because the NaH-meditated H/D exchange is not involved in the catalytic cycle, whether or not the NaH-mediated H/D exchange takes place, the mechanisms-A and -B remain the same, and thus our conclusions hold true.

Both mechanisms can explain the deuteration on the C^{α} atom of amide product **4a** (eq 4), because the two mechanisms transfer the D^{α} atoms of **2a** to the Ru-center via the TSs (**TS5** and **TS13**/**TS14** in both mechanisms), and the C^{α} atom of **4a** obtains the D atom via **TS1**. However, both mechanisms do not activate the $C^{\alpha}-H^{\alpha}$ bond of nitrile **3** and thus cannot rationalize the deuteration on C^{β} of **4a**. Hong et al. presumed that NaH may mediate the deuteration on the C^{β} atom of **4a**. We noticed that their D-labeling experiment was carried out under the optimal conditions, using NHC precursor and NaH to produce the NHC ligand. They also run the reaction using **6** as a catalyst precursor prepared separately (without using NaH and NHC precursor). Thus, a D-labeling experiment using **6** as the mediator would help clarify the role of NaH in the deuteration of $C^{\beta}H$ and NH of **4a**.

As our mechanism-B involves alcohol as a reductant in nitrile hydrogenation, Hong et al. reported that in the absence of alcohol, they observed NMR signals for Ru-bond imine and free imine. Our mechanism-B does not contradict the experiment, because **8** reacting with imine is energetically feasible (see the black pathway in Scheme 2) without using alcohol.

Compared to the borrowing hydrogen strategy in DHC/BHM reactions (Scheme 1A), the way of borrowing hydrogen in the present case is different. In DHC/BHM reactions, one substrate (e.g., alcohol) first gives two hydrogen atoms to the catalyst via dehydrogenation, forming the catalyst-H_2 hydride, then the two H atoms in catalyst-H_2 transfer to the coupling partner or form H_2 being released. In the present reaction, the alcohol substrate only transfers its H^{α} atom to the catalyst **8**, and its H^{OH} atom is transferred to the nitrile partner directly.

4. CONCLUSIONS

In summary, we have performed a DFT mechanistic study to understand the redox-neutral amide synthesis from primary alcohol and nitrile. The study shows that the reaction is catalyzed by $Ru^{II}H_2(CO)(PPh_3)(I^iPr)$ (I^iPr = 1,2-diisopropylimidazol-2-ylidene) actual catalyst via four stages: nitrile reduction, alcohol dehydrogenation, C−N coupling, and amide release via β-H elimination. Generally, the alcohol dehydrogenation in dehydrogenative coupling (DHC)/or hydrogen borrowing methodology (HBM) takes place separately, transferring H^{α} and hydroxyl H^{OH} to the catalyst to form the catalyst-H_2 hydride. Differently, the alcohol dehydrogenation in the present reactions couples with nitrile hydrogenation, alcohol playing a reductant role to aid nitrile reduction to transfer its H^{α} to the catalyst and the H^{OH} atom directly to nitrile N atom. In our computed mechanism (i.e., mechanism-B), the Ru^{II} state of the active catalyst is retained in the whole catalytic cycle, which is different from mechanism-A postulated by experimentalists which involves Ru^{II}/Ru^{0} redox manifold and the Ru^{0} complex performing alcohol dehydrogenation independently. As a consequence, mechanism-B is energetically more favorable than mechanism-A. In mechanism-B, the (N-)H atom of the amide bond exclusively originates from the hydroxyl H^{OH} atom of alcohol. In comparison, the (N-)H atom in mechanism-A comes from either H^{OH} or H^{α} of alcohol. The methodology of borrowing hydrogen, used by nitrile via participating in alcohol dehydrogenation is different from that in the DHC/BHM reactions. We expect that the mechanism could be the basis to develop new routes for utilization of DHC and HBM methodology.

■ ASSOCIATED CONTENT

Supporting Information

Additional computational results, total energies, and Cartesian coordinates of all optimized structures. This material is available free of charge via the Internet at http://pubs.acs.org.

■ AUTHOR INFORMATION

Corresponding Author

*E-mail: zxwang@ucas.ac.cn

Notes

The authors declare no competing financial interest.

■ ACKNOWLEDGMENTS

This work is financially supported by National Natural Science Foundation of China (Nos. 21173263 and 21373216).

■ REFERENCES

(1) (a) Anastas, P. T., Warner, J. C. *Green Chemistry: Theory and Practice*; Oxford University Press; Oxford, England; New York, 1998. (b) Clark, J. H. *Green Chem.* **1999**, *1*, 1−8. (c) Anastas, P. T.; Kirchhoff, M. M. *Acc. Chem. Res.* **2002**, *35*, 686−694. (d) Poliakoff, M.; Fitzpatrick, J. M.; Farren, T. R.; Anastas, P. T. *Science* **2002**, *297*, 807−810. (e) Horváth, I. T.; Anastas, P. T. *Chem. Rev.* **2007**, *107*, 2167−2168. (f) Tsarevsky, N. V.; Matyjaszewski, K. *Chem. Rev.* **2007**, *107*, 2270−2299.

(2) (a) Blum, Y.; Shvo, Y. *J. Organomet. Chem.* **1985**, *282*, C7−C10. (b) Murahashi, S.; Naota, T.; Ito, K.; Maeda, Y.; Taki, H. *J. Org. Chem.* **1987**, *52*, 4319−4327. (c) Zhang, J.; Leitus, G.; Ben-David, Y.; Milstein, D. *J. Am. Chem. Soc.* **2005**, *127*, 10840−10841.

(3) (a) Friedrich, A.; Schneider, S. *ChemCatChem.* **2009**, *1*, 72−73. (b) Dobereiner, G. E.; Crabtree, R. H. *Chem. Rev.* **2009**, *110*, 681−703. (c) Johnson, T. C.; Morris, D. J.; Wills, M. *Chem. Soc. Rev.* **2010**, *39*, 81−88. (d) Watson, A. J.; Williams, J. M. *Science* **2010**, *329*, 635−636. (e) Choi, J.; MacArthur, A. H.; Brookhart, M.; Goldman, A. S. *Chem. Rev.* **2011**, *111*, 1761−1779. (f) Gunanathan, C.; Milstein, D. *Acc. Chem. Res.* **2011**, *44*, 588−602. (g) Marr, A. C. *Catal. Sci. Technol.* **2012**, *2*, 279−287. (h) Gunanathan, C.; Milstein, D. *Science* **2013**, *341*, 249−260. (i) Zeng, G.; Sakaki, S.; Fujita, K.-i.; Sano, H.; Yamaguchi, R. *ACS Catal.* **2014**, *4*, 1010−1020. (j) Chakraborty, S.; Brennessel, W. W.; Jones, W. D. *J. Am. Chem. Soc.* **2014**, *136*, 8564−8567.

(4) (a) Hamid, M. H. S. A.; Allen, C. L.; Lamb, G. W.; Maxwell, A. C.; Maytum, H. C.; Watson, A. J.; Williams, J. M. *J. Am. Chem. Soc.* **2009**, *131*, 1766−1774. (b) Miao, L.; Dimaggio, S. C.; Shu, H.; Trudell, M. L. *Org. Lett.* . **2009**, *11*, 1579−1582. (c) Berliner, M. A.; Dubant, S. P. A.; Makowski, T.; Ng, K.; Sitter, B.; Wager, C.; Zhang, Y. *Org. Process Res. Dev.* **2011**, *15*, 1052−1062. (d) Guillena, G.; Ramón, D. J.; Yus, M. *Chem. Rev.* **2010**, *110*, 1611−1641.

(5) (a) Gunanathan, C.; Ben-David, Y.; Milstein, D. *Science* **2007**, *317*, 790−792. (b) Nordstrøm, L. U.; Vogt, H.; Madsen, R. *J. Am. Chem. Soc.* **2008**, *130*, 17672−17673. (c) Chen, C.; Zhang, Y.; Hong, S. H. *J. Org. Chem.* **2011**, *76*, 10005−10010.
(6) (a) Gnanaprakasam, B.; Zhang, J.; Milstein, D. *Angew. Chem., Int. Ed.* **2010**, *49*, 1468−1471. (b) He, L.-P.; Chen, T.; Gong, D.; Lai, Z.-P.; Huang, K.-W. *Organometallics* **2012**, *31*, 5208−5211.
(7) (a) Gunanathan, C.; Shimon, L. J. W.; Milstein, D. *J. Am. Chem. Soc.* **2009**, *131*, 3146−3147. (b) Spasyuk, D.; Smith, S.; Gusev, D. G. *Angew. Chem., Int. Ed.* **2012**, *51*, 2772−2775. (c) Nielsen, M.; Junge, H.; Kammer, A.; Beller, M. *Angew. Chem., Int. Ed.* **2012**, *51*, 5711−5713. (d) Kossoy, E.; Diskin-Posner, Y.; Leitus, G.; Milstein, D. *Adv. Synth. Catal.* **2012**, *354*, 497−504. (e) Zeng, G.; Chen, T.; He, L.-P; Pinnau, I.; Lai, Z.-P.; Huang, K.-W. *Chem.—Eur. J.* **2012**, *18*, 15940−15943.
(8) (a) Schley, N. D.; Dobereiner, G. E.; Crabtree, R. H. *Organometallics* **2011**, *30*, 4174−4179. (b) Srimani, D.; Ben-David, Y.; Milstein, D. *Angew. Chem., Int. Ed.* **2013**, *52*, 4012−4015. (c) Zhang, M.; Fang, X.; Neumann, H.; Beller, M. *J. Am. Chem. Soc.* **2013**, *135*, 11384−11388.
(9) Goldman, A. S.; Roy, A. H.; Huang, Z.; Ahuja, R.; Schinski, W.; Brookhart, M. *Science.* **2006**, *312*, 257−261.
(10) (a) Humphrey, J. M.; Chamberlin, A. R. *Chem. Rev.* **1997**, *97*, 2243−2266. (b) Valeur, E.; Bradley, M. *Chem. Soc. Rev.* **2009**, *38*, 606−631. (c) Pattabiraman, V. R.; Bode, J. W. *Nature* **2011**, *480*, 471−479. (d) Crespo, L.; Sanclimens, G.; Pons, M.; Giralt, E.; Royo, M.; Albericio, F. *Chem. Rev.* **2005**, *105*, 1663−1681.
(11) Wieland, T.; Bodanszky, M. *The World of Peptides:A Brief History of Peptide Chemistry*; Springer: New York, 1991.
(12) (a) Bode, J. W.; Opin, Curr. *Drug Discovery Dev.* **2006**, *9*, 765−775. (b) Carey, J. S.; Laffan, D.; Thomson, C.; Williams, M. T. *Org. Biomol. Chem.* **2006**, *4*, 2337−2347.
(13) (a) Gololobov, Y. G.; Kasukhin, L. F. *Tetrahedron.* **1992**, *48*, 1353−1406. (b) Saxon, E.; Bertozzi, C. R. *Science.* **2000**, *287*, 2007−2010. (c) Pianowski, Z.; Gorska, K.; Oswald, L.; Merten, C. A.; Winssinger, N. *J. Am. Chem. Soc.* **2009**, *131*, 6492−6497.
(14) (a) Lang, S.; Murphy, J. A. *Chem. Soc. Rev.* **2006**, *35*, 146−156. (b) Ribelin, T.; Katz, C. E.; English, D. G.; Smith, S.; Manukyan, A. K.; Day, V. W.; Neuenswander, B.; Poutsma, J. L.; Aub, J. *Angew. Chem., Int. Ed.* **2008**, *47*, 6233−6235.
(15) (a) Owston, N. A.; Parker, A. J.; Williams, J. M. J. *Org. Lett.* **2007**, *9*, 3599−3601. (b) Hashimoto, M.; Obora, Y.; Sakaguchi, S.; Ishii, Y. *J. Org. Chem.* **2008**, *73*, 2894−2897.
(16) (a) Ghosh, S. C.; Muthaiah, S.; Zhang, Y.; Xu, X.; Hong, S. H. *Adv. Synth. Catal.* **2009**, *351*, 2643−2649. (b) Watson, A. J. A.; Maxwell, A. C.; Williams, J. M. *J. Org. Lett.* **2009**, *11*, 2667−2670. (c) Zhang, Y.; Chen, C.; Ghosh, S. C.; Li, Y.; Hong, S. H. *Organometallics* **2010**, *29*, 1374−1378. (d) Dam, J. H.; Osztrovszky, G.; Nordstrom, L. U.; Madsen, R. *Chem.—Eur. J.* **2010**, *16*, 6820−6827. (e) Muthaiah, S.; Ghosh, S. C.; Jee, J. E.; Chen, C.; Zhang, J.; Hong, S. H. *J. Org. Chem.* **2010**, *75*, 3002−3006. (f) Chen, C.; Hong, S. H. *Org. Biomol. Chem.* **2011**, *9*, 20−26. (g) Ghosh, S. C.; Hong, S. H. *Eur. J. Org. Chem.* **2010**, *2010*, 4266−4270. (h) Zhang, J.; Senthilkumar, M.; Ghosh, S. C.; Hong, S. H. *Angew. Chem., Int. Ed.* **2010**, *49*, 6391−6395. (i) Makarov, I. S.; Fristrup, P.; Madsen, R. *Chem.—Eur. J.* **2012**, *18*, 15683−15692. (j) Saha, B.; Sengupta, G.; Sarbajna, A.; Dutta, I.; Bera, J. K. *J. Organomet. Chem.* **2013**, *12*, 051−057.
(17) Reddy, K. R.; Maheswari, C. U.; Venkateshwar, M.; Kantam, M. L. *Eur. J. Org. Chem.* **2008**, *2008*, 3619−3662.
(18) Zweifel, T.; Naubron, J.-V.; Gr€utzmacher, H. *Angew. Chem., Int. Ed.* **2009**, *48*, 559−563.
(19) Nova, A.; Balcells, D.; Schley, N. D.; Dobereiner, G. E.; Crabtree, R. H.; Eisenstein, O. *Organometallics* **2010**, *29*, 6548−6558.
(20) Shimizu, K.; Ohshima, K.; Satsuma, A. *Chem.—Eur. J.* **2009**, *15*, 9977−9980.
(21) Zeng, H.; Guan, Z. *J. Am. Chem. Soc.* **2011**, *133*, 1159−1161.
(22) (a) Niu, S.; Hall, M. B. *J. Am. Chem. Soc.* **1999**, *121*, 3992−3999. (b) Krogh-Jespersen, K.; Czerw, M.; Summa, N.; Renkema, K. B.; Achord, P. D.; Goldman, A. S. *J. Am. Chem. Soc.* **2002**, *124*, 11404−11416. (c) Cui, X.; Fan, Y.; Hall, M. B.; Burgess, K. *Chem.—Eur. J.* **2005**, *11*, 6859−6868. (d) Balcells, D.; Nova, A.; Clot, E.; Gnanamgari, D.; Crabtree, R. H.; Eisenstein, O. *Organometallics* **2008**, *27*, 2529−2535. (e) Iron, M. A.; Ben-Ari, E.; Cohen, R.; Milstein, D. *Dalton Trans* **2009**, 9433−9439. (f) Yang, X.; Hall, M. B. *J. Am. Chem. Soc.* **2010**, *132*, 120−130. (g) Zimmerman, P. M.; Paul, A.; Zhang, Z.; Musgrave, C. B. *Angew. Chem., Int. Ed.* **2009**, *48*, 2201−2205. (h) Schwartsburd, L.; Iron, M. A.; Konstantinovski, L.; Diskin-Posner, Y.; Leitus, G.; Shimon, L. J. W.; Milstein, D. *Organometallics* **2010**, *29*, 3817−3827. (i) Zeng, G.; Li, S. *Inorg. Chem.* **2011**, *50*, 10572−10580. (j) Yang, X. *ACS Catal.* **2012**, *2*, 964−970. (k) Cho, D.; Ko, K. C.; Lee, J. Y. *Organometallics* **2013**, *32*, 4571−4576. (l) Yang, X. *ACS Catal.* **2013**, 2684−2688. (m) Li, H.; Hall, M. B. *J. Am. Chem. Soc.* **2013**, *136*, 383−395. (n) Sandhya, K. S.; Suresh, C. H. *Organometallics* **2013**, *32*, 2926−2933.
(23) (a) Li, H.; Wang, X.; Huang, F.; Lu, G.; Jiang, J.; Wang, Z.-X. *Organometallics* **2011**, *30*, 5233−5247. (b) Li, H.; Lu, G.; Jiang, J.; Huang, F.; Wang, Z.-X. *Organometallics* **2011**, *30*, 2349−2363. (c) Li, H.; Jiang, J.; Lu, G.; Huang, F.; Wang, Z.-X. *Organometallics* **2011**, *30*, 3131−3141. (d) Li, H.; Wen, M.; Wang, Z. X. *Inorg. Chem.* **2012**, *51*, 5716−5727. (e) Li, H.; Wang, X.; Wen, M.; Wang, Z.-X. *Eur. J. Inorg. Chem.* **2012**, *2012*, 5011−5020. (f) Li, H.; Wang, Z. *Sci. China - Chem.* **2012**, *55*, 1991−2008. (g) Qu, S.; Dang, Y.; Song, C.; Wen, M.; Huang, K.; Wang, Z.-X. *J. Am. Chem. Soc.* **2014**, *136*, 4974−4991.
(24) Gnanaprakasam, B.; Balaraman, E.; Ben-David, Y.; Milstein, D. *Angew. Chem., Int. Ed.* **2011**, *50*, 12240−12244.
(25) Michlik, S.; Kempe, R. *Nat. Chem.* **2013**, *5*, 140−144.
(26) Kang, B.; Fu, Z.; Hong, S. H. *J. Am. Chem. Soc.* **2013**, *135*, 11704−11707.
(27) (a) Lee, C. T.; Yang, W. T.; Parr, R. G. *Phys. Rev. B* **1988**, *37*, 785−789. (b) Becke, A. D. *J. Chem. Phys.* **1993**, *98*, 5648−5652.
(28) (a) Andrae, D.; Haussermann, U.; Dolg, M.; Stoll, H.; Preuss, H. *Theor. Chem. Acc.* **1990**, *77*, 123−141. (b) Roy, L. E.; Hay, P. J.; Martin, R. L. *J. Chem. Theory Comput.* **2008**, *4*, 1029−1031.
(29) (a) Hehre, W. J.; Ditchfield, R.; Pople, J. A. *J. Chem. Phys.* **1972**, *56*, 2257−2261. (b) Harihara, Pc; Pople, J. A. *Theor. Chem. Acc.* **1973**, *28*, 213−222. (c) Harihara, Pc; Pople, J. A. *Mol. Phys.* **1974**, *27*, 209−214. (d) Gordon, M. S. *Chem. Phys. Lett.* **1980**, *76*, 163−168.
(30) (a) Zhao, Y.; Truhlar, D. G. *Acc. Chem. Res.* **2008**, *41*, 157−167. (b) Sliwa, P.; Handzlik, J. *Chem. Phys. Lett.* **2010**, *493*, 273−278. (c) Zhao, Y.; Truhlar, D. G. *J. Chem. Theory Comput.* **2009**, *5*, 324−333. (d) Kulkarni, A. D.; Truhlar, D. G. *J. Chem. Theory Comput.* **2011**, *7*, 2325−2332.
(31) Marenich, A. V.; Cramer, C. J.; Truhlar, D. G. *J. Phys. Chem. B* **2009**, *113*, 6378−6396.
(32) (a) Hay, P. J. *J. Chem. Phys.* **1977**, *66*, 4377−4384. (b) Krishnan, R.; Binkley, J. S.; Seeger, R.; Pople, J. A. *J. Chem. Phys.* **1980**, *72*, 650−654. (c) Francl, M. M.; Pietro, W. J.; Hehre, W. J.; Binkley, J. S.; Gordon, M. S.; DeFrees, D. J.; Pople, J. A. *J. Chem. Phys.* **1982**, *77*, 3654−3665. (d) Clark, T.; Chandrasekhar, J.; Spitznagel, G. W.; Schleyer, P. V. R. *J. Comput. Chem.* **1983**, *4*, 294−301. (e) Frisch, M. J.; Pople, J. A.; Binkley, J. S. *J. Chem. Phys.* **1984**, *80*, 3265−3269. (f) Raghavachari, K.; Trucks, G. W. *J. Chem. Phys.* **1989**, *91*, 1062−1065. (g) Binning, R. C.; Curtiss, L. A. *J. Comput. Chem.* **1990**, *11*, 1206−1216.
(33) (a) Tang, S.-Y.; Guo, Q.-X.; Fu, Y. *Chem.—Eur. J.* **2011**, *17*, 13866−13876. (b) Giri, R.; Lan, Y.; Liu, P.; Houk, K. N.; Yu, J.-Q. *J. Am. Chem. Soc.* **2012**, *134*, 14118−14126. (c) Herbert, M. B.; Lan, Y.; Keitz, B. K.; Liu, P.; Endo, K.; Day, M. W.; Houk, K. N.; Grubbs, R. H. *J. Am. Chem. Soc.* **2012**, *134*, 7861−7866. (d) Dang, Y.; Wang, Z.-X.; Wang, X. *Organometallics* **2012**, *31*, 7222−7234.
(34) (a) Yu, Z. X.; Houk, K. N. *J. Am. Chem. Soc.* **2003**, *125*, 13825−13830. (b) Liang, Y.; Liu, S.; Xia, Y.; Li, Y.; Yu, Z.-X. *Chem.—Eur. J.* **2008**, *14*, 4361−4373. (c) Huang, D.; Makhlynets, O. V.; Tan, L. L.; Lee, S. C.; Rybak-Akimova, E. V.; Holm, R. H. *Proc. Natl. Acad. Sci. U.S.A.* **2011**, *108*, 1222−1227. (d) Huang, D.; Makhlynets, O. V.; Tan, L. L.; Lee, S. C.; Rybak-Akimova, E. V.; Holm, R. H. *Inorg. Chem.* **2011**, *50*, 10070−10081.

(35) Martin, R. L.; Hay, P. J.; Pratt, L. R. *J. Phys. Chem. A* **1998**, *102*, 3565−3573.
(36) Wen, M.; Huang, F.; Lu, G.; Wang, Z.-X. *Inorg. Chem.* **2013**, *52*, 12098−12107.
(37) Frisch, M. J.; Trucks, G. W.; Schlegel, H. B.; Scuseria, G. E.; Robb, M. A.; Cheeseman, J. R.; Scalmani, G.; Barone, V.; Mennucci, B.; Petersson, G. A.; Nakatsuji, H.; Caricato, M.; Li, X.; Hratchian, H. P.; Izmaylov, A. F.; Bloino, J.; Zheng, G.; Sonnenberg, J. L.; Hada, M.; Ehara, M.; Toyota, K.; Fukuda, R.; Hasegawa, J.; Ishida, M.; Nakajima, T.; Honda, Y.; Kitao, O.; Nakai, H.; Vreven, T.; Montgomery, J. A., Jr.; Peralta, J. E.; Ogliaro, F.; Bearpark, M.; Heyd, J. J.; Brothers, E.; Kudin, K. N.; Staroverov, V. N.; Kobayashi, R.; Normand, J.; Raghavachari, K.; Rendell, A.; Burant, J. C.; Iyengar, S. S.; Tomasi, J.; Cossi, M.; Rega, N.; Millam, J. M.; Klene, M.; Knox, J. E.; Cross, J. B.; Bakken, V.; Adamo, C.; Jaramillo, J.; Gomperts, R.; Stratmann, R. E.; Yazyev, O.; Austin, A. J.; Cammi, R.; Pomelli, C.; Ochterski, J. W.; Martin, R. L.; Morokuma, K.; Zakrzewski, V. G.; Voth, G. A.; Salvador, P.; Dannenberg, J. J.; Dapprich, S.; Daniels, A. D.; Farkas, O.; Foresman, J. B.; Ortiz, J. V.; Cioslowski, J.; Fox, D. J. *Gaussian 09*, Revision A.01; Gaussian, Inc.: Wallingford CT, 2009.
(38) (a) Erdtman, E.; Bushnell, E. A. C.; Gauld, J. W.; Eriksson, L. A. *Comput. Theor. Chem.* **2011**, *963*, 479−489. (b) Qu, S.; Dang, Y.; Wen, M.; Wang, Z.-X. *Chem.—Eur. J.* **2013**, *19*, 3827−3832.